8B.5 A HYBRID NUDGING-EnKF APPROACH TO DATA ASSIMILATION

Lili Lei* and David R. Stauffer

Pennsylvania State University, University Park, Pennsylvania

1. INTRODUCTION

Operational weather analysis and numerical weather prediction (NWP) has evolved from use of only standard surface and upper-air observations towards assimilation of many additional data sources from surface mesonets, satellites and radars. Data assimilation is the process used to determine a more accurate state of atmosphere from these diverse observations and model forecast / background fields. The nudging data assimilation scheme has become increasingly popular for mesoscale data assimilation because of its efficiency and its use of the full set of model equations. This continuous assimilation method allows the corrections to be made gradually thereby reducing insertion shock common with other intermittent methods while allowing them to influence other variables and future time periods through the model equations' interactions (Stauffer and Seaman 1990, Stauffer and Seaman 1994).

The ensemble Kalman filter (EnKF), on the other hand, takes advantage of ensemble forecasts, which are becoming more widely available, to get flow-dependent background error covariance which can be used to spread the corrections and more efficiently seek the optimum state between the model background and the observations (Evensen 1994). Although the nudging scheme is computationally efficient, it is often used with ad-hoc nudging coefficients based on theory and past experience but they can be better specified by adjoints and/or model statistics (e.g., Stauffer and Bao 1993). The EnKF includes both dynamic and statistical information but is computationally expensive. Thus a hybrid nudging-EnKF approach with potential use for NWP is proposed and explored here using the non-linear Lorenz (1963) three-variable model system, which allows the EnKF to provide flow-dependent / time-varying error covariance to compute the nudging coefficient matrix and to further correct the model fields.

* *Corresponding author address:* Lili Lei, Department of Meteorology, 503 Walker Building, Pennsylvania State University, University Park, PA 16803-5013; e-mail: lzl130@psu.edu.

2. METHODOLOGY FOR HYBRID NUDGING-EnKF APPROACH

To describe our proposed data assimilation system, we write the equations of the system as:

$$\frac{d\,\vec{\mathrm{x}}}{dt} = f\left(\vec{\mathrm{x}}\right) + \mathrm{G}\cdot \mathrm{w}\cdot\left(\vec{\mathrm{x}}^{o} - \vec{\mathrm{x}}\right), \qquad (1)$$

where $\vec{\mathrm{x}}$ and f are the state vector and standard forcing function of the system respectively, $\vec{\mathrm{x}}^{o}$ is observation, G is the nudging magnitude matrix for the nudging term and w is generally the nudging spatial-temporal weighting coefficient used to map the innovation (observation minus the model background) in observation space and time to the model grid cell and time step. The product of G and w is defined here as the nudging coefficient.

The traditional nudging data assimilation scheme sets the nudging coefficient with non-zero diagonal elements and zero off-diagonal elements so that the nudging term is relatively small compared to the other physical terms $f\left(\vec{\mathrm{x}}\right)$. The nudging coefficient is often specified by past experience and experimentation (e.g., Stauffer and Seaman 1994) to emulate the error covariance or correlation in the error at the observation location with that in a spatial and temporal region / window about the observation site and observation time. To determine flow-dependent / time-dependent nudging coefficients, the hybrid nudging-EnKF method uses the gain matrix of the EnKF to compute the nudging magnitude matrix (Kalata 1984; Painter et al. 1990; Yang et al. 2006).

The gain matrix of the EnKF is (Evensen 1994):

$$\mathrm{K} = \mathrm{B}\,\mathrm{H}^{\mathrm{T}}\left(\mathrm{H}\,\mathrm{B}\,\mathrm{H}^{\mathrm{T}} + \mathrm{R}\right)^{-1}, \qquad (2)$$

where B is the covariance matrix of background errors, R is covariance matrix of observation error, and H is the observation operator. In the application presented in this paper, the nudging magnitude matrix G is a function of EnKF gain matrix and nudging weighting coefficient w. The nudging magnitude matrix in the hybrid nudging-EnKF method is defined as:

$$\mathrm{G} = t_{w}\,\mathrm{K}, \qquad (3)$$

where t_w is a function of the nudging weighting coefficient.

Compared to the traditional nudging approach, the hybrid nudging-EnKF approach takes advantage of ensemble forecasts which offer flow-dependent / time-dependent background error covariance to provide a flow-dependent / time-varying nudging coefficient. The hybrid nudging-EnKF approach can also extend the nudging magnitude matrix from having non-zero diagonal elements and zero off-diagonal elements to a full non-zero matrix. This may lead to more accurate adjustment of background to observation than the traditional approach.

3. MODEL DESCRIPTION AND EXPERIMENTAL DESIGN

As a test bed for data assimilation, the non-linear Lorenz (1963) three-variable model system consisting of three coupled and nonlinear ordinary differential equations is applied here:

$$\begin{aligned} \frac{dx}{dt} &= \sigma(y-x) \\ \frac{dy}{dt} &= rx - y - xz \\ \frac{dz}{dt} &= xy - bz \ , \end{aligned} \tag{4}$$

where the parameters are set as standard values: σ =10, r =28, b =8/3, and model error is not considered (i.e., perfect model assumption). The state vector $\vec{\mathrm{x}}$ and observation vector $\vec{\mathrm{x}}^o$ in Eq. (1) are now column vectors with dimension 3×1, and the nudging magnitude matrix G and the EnKF gain matrix K are dimensioned 3×3.

We integrate the Lorenz model in time using a fourth-order Runge-Kutta numerical scheme and a time step Δt of 0.01. Equation (4) is integrated from a true initial value set as (1.508870, -1.531271, 5.46091) to obtain the true state. For the simulated observations, we add the observation errors chosen randomly from a Gaussian distribution with mean zero and variance 1.0 to the true values from the true state at corresponding times. Since the true initial value is unknown in the real atmosphere, a central initial value, defined as the ensemble mean at the initial time step, is assumed to be an approximate true initial value, which is the true initial value with an additive random error. By adding random errors from a Gaussian distribution with mean zero and variance 1.0 to the central initial value, the initial values for the ensemble are derived. The number of ensemble members is set to 100. To eliminate the effects of transients (Yang et al. 2006), we integrate the Lorenz model from the central initial value and the ensemble for 1000 time steps first and then assimilate the observations by either the traditional nudging method, the EnKF, or variations of the hybrid nudging-EnKF approach. The integration from the central initial value is called as central state in the following. The observation density is one per 25 time steps by default, and is varied to one per 10 and one per 50 time steps in two experiments.

For the hybrid nudging-EnKF approach, the system (Eq. (4)) becomes:

$$\begin{aligned} \frac{dx}{dt} &= \sigma(y-x) + g_{xx}\cdot \mathrm{w}\cdot(x^0 - x) + \\ &\quad g_{xy}\cdot \mathrm{w}\cdot(y^0 - y) + g_{xz}\cdot \mathrm{w}\cdot(z^0 - z) \\ \frac{dy}{dt} &= rx - y - xz + g_{yx}\cdot \mathrm{w}\cdot(x^0 - x) + \\ &\quad g_{yy}\cdot \mathrm{w}\cdot(y^0 - y) + g_{yz}\cdot \mathrm{w}\cdot(z^0 - z) \\ \frac{dz}{dt} &= xy - bz + g_{zx}\cdot \mathrm{w}\cdot(x^0 - x) + \\ &\quad g_{zy}\cdot \mathrm{w}\cdot(y^0 - y) + g_{zz}\cdot \mathrm{w}\cdot(z^0 - z) \end{aligned} \ , \tag{5}$$

where each g is an element in the nudging magnitude matrix G in Eq. (1). The traditional nudging approach has non-zero diagonal elements and zero off-diagonal elements in the nudging magnitude matrix.

For both the traditional nudging method and the hybrid nudging-EnKF methods applied to the Lorenz three-variable system, the nudging weighting coefficient w only varies in time as defined by (Stauffer and Seaman 1990):

$$\mathrm{w} = \mathrm{w}_t = \begin{cases} 1, & t \in \left[t^o - \tau/2, t^o + \tau/2\right] \\ \left(\tau - \left|t - t^o\right|\right)/(\tau/2), & \\ \quad t \in \left[t^o - \tau, t^o - \tau/2\right] \cup \left[t^o + \tau/2, t^o + \tau\right] & \\ 0, & \textit{otherwise} \end{cases} , \tag{6}$$

where t is the model time, t^o is the observation time, and τ is the half-period of the nudging time window. Given τ and w, the function t_w in Eq. (3) is:

$$\mathrm{t}_w = 1 \Big/ \left(\sum_{i=t^o-\tau}^{t^o} \mathrm{w}\cdot\Delta t \right). \tag{7}$$

Since the nudging weighting coefficients is fixed as description of Eq. (6), t_w is a function of the half-period τ and time step Δt as shown in Eq. (7).

In the traditional nudging approach (named TNGAx, where x is the value of the half-period of the

nudging time window, 8, 4, 2 and 1), the diagonal elements of G are set to 10.0 (Yang et al. 2006). After the initial integration of 1000 time steps, we continue to integrate the central state forward in time by assimilating the observations using traditional nudging for another 3000 time steps. This and the following experiments are also integrated for a second 3000-step period from 4000 to 7000 time steps. The second experiment, which integrates the ensemble forward and assimilates observations by the EnKF, is named as EKFA. The HNKFx (HNKDx) experiment uses the full nudging magnitude matrix (diagonal elements only) and assimilates the observations by the hybrid nudging-EnKF approach in the central state while the nudging magnitude matrix G is determined by creating an ensemble by adding random errors to the central value at one observation time step and integrating the ensemble from this observation time to the next observation time. Then we calculate the results of the average root mean square (RMS) errors of the central state (TNGAx, HNKFx and HNKDx) and the ensemble mean (EKFA) compared to the truth for all three variables together every time step during the 3000 time steps. The FCST or control experiment is the result of integrating the model forward for 3000 time steps without assimilating any observations.

For experiments HNKFx and HNKDx, we test the hypothesis that a temporally averaged nudging coefficient may be computed for the first 3000-step period and then frozen for use in these experiments (FHNKFx and FHNKDx) during the first 3000-step period and again for a future 3000-step period.

4. PRELIMINARY RESULTS

During the first 3000-step period, the results of FCST, EKFA, TNGAx, HNKFx and HNKDx are shown in Table 1. All data assimilation schemes produce much smaller RMS analysis errors than the control FCST without data assimilation, 17.9. The EKFA shows the smallest RMS analysis error (1.2). Both hybrid nudging-EnKF approaches (one with the full nudging magnitude matrix and the other with diagonal elements only) generally have smaller RMS errors than the traditional nudging, since these two hybrid approaches use the ensemble spread to estimate the background error information and use this in the nudging coefficients. The hybrid methods can produce RMS errors that are only slightly larger than the EnKF. Also, the RMS errors using the full nudging magnitude matrix are smaller than those using diagonal elements only.

The hybrid nudging-EnKF with only diagonal elements of the nudging magnitude matrix (see Eq. (5)) still improves the statistical scores compared to the traditional nudging method by using the EnKF to provide time varying nudging coefficients that may be larger or smaller than the traditional nudging coefficient of 10. Furthermore, the hybrid nudging-

	RMS		RMS		RMS		RMS
FCST	17.9	TNGA8	2.1	HNKF8/HNKD8	1.8/2.2	FHNKF8/FHNKD8	2.1/2.8
EKFA	1.2	TNGA4	2.5	HNKF4/HNKD4	1.3/1.9	FHNKF4/FHNKD4	1.8/2.6
		TNGA2	7.2	HNKF2/HNKD2	1.3/2.1	FHNKF2/FHNKD2	1.9/2.9
		TNGA1	15.7	HNKF1/HNKD1	1.5/1.8	FHNKF1/FHNKD1	1.6/2.3

Table 1. The average RMS error in the first 3000-step period of the no data assimilation control experiment FCST, EnKF data assimilation experiment EKFA, traditional nudging data assimilation experiments TNGAx, hybrid nudging-EnKF data assimilation experiments HNKFx and HNKDx, and frozen hybrid nudging-EnKF data assimilation experiments FHNKFx and FHNKDx, respectively.

	RMS		RMS		RMS
FCST	18.0	TNGA8	2.7	FHNKF8/FHNKD8	2.4/3.3
EKFA	1.4	TNGA4	3.5	FHNKF4/FHNKD4	2. 6/3.7
		TNGA2	10.9	FHNKF2/FHNKD2	2.8/4.0
		TNGA1	10.8	FHNKF1/FHNKD1	2.2/3.4

Table 2. The average RMS error in the second 3000-step period of the no data assimilation control experiment FCST, EnKF data assimilation experiment EKFA, traditional nudging data assimilation experiments TNGAx, and frozen hybrid nudging-EnKF data assimilation experiments FHNKFx and FHNKDx, respectively.

EnKF with the full nudging magnitude matrix (Eq. (5)) extends the nudging magnitude matrix from only non-zero diagonal elements and zero off-diagonal elements matrix to a full non-zero matrix. Figure 1 shows the average value of the nudging coefficients in the first 3000-step period of HNKF4. The diagonal nudging coefficients are larger than the off-diagonal ones in the y and z equations, and the off-diagonal nudging coefficients relating to variable z are much smaller than those off-diagonal elements of x and y. These findings are consistent with the results of Yang et al. (2006). The use of the EnKF gain matrix to provide information to the nudging coefficients has been proven. The diagonal nudging coefficients are always positive since they are computed from the variance of the background and they determine the e-folding time for reducing the errors of the system. However, the off-diagonal nudging coefficients may be negative, like the ones of variable z (Fig. 1), because they are based on the covariance of the background which may be negative. The off-diagonal nudging coefficients have no direct effect on the e-folding time of the system.

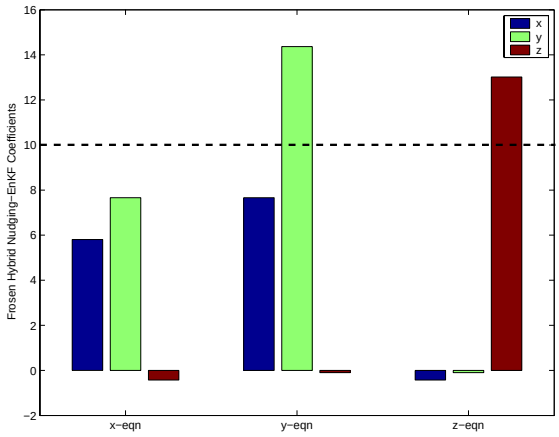

Figure 1. The average (frozen) hybrid nudging-EnKF coefficients in the first 3000-step period in each equation in HNKF4. The dashed line denotes the nudging coefficient magnitude of the traditional nudging approach applied here.

Because the hybrid nudging-EnKF approach with the full nudging magnitude matrix obtains better results than that with the diagonal elements only, the off-diagonal nudging coefficients play an important role in further reducing the RMS error although they are small. The Lorenz system with three variables can be seen as a trajectory of a particle in a three-dimensional space: we can see that the effects of the off-diagonal nudging coefficients offer a more accurate direction and magnitude of forcing on the particle from the background towards the observation, which leads to faster and more accurate interaction between the background and the observation and smaller RMS errors. This may be the reason that using the full nudging magnitude matrix produces better results than using the diagonal elements only.

Since running ensembles and applying the EnKF can be quite expensive in real-time NWP applications, we wanted to determine proof of concept that historical nudging coefficients from hybrid nudging-EnKF schemes can be effective in future data assimilations. We have rerun the previous HNKFx and HNKDx experiments with time invariant (frozen) nudging coefficients based on the temporally averaged values of the previous experiments to create FHNKFx and FHNKDx, in the first and second 3000-step periods. The frozen nudging coefficients of FHNKF4 are temporally averaged from HNKF4 and are shown in Fig. 1. The results of FHNKFx and FHNKDx during the first 3000-step period are also shown in Table 1. The average RMS analysis errors of FHNKFx and FHNKDx are somewhat larger than HNKFx and HNKDx respectively, but are generally similar or smaller to those from TNGAx. When the half-period of the nudging time window decreases (to x=2 or x=1), the FHNKFx and FHNKDx get much better results than the TNGAx. This is likely because the nudging coefficients have become much larger in magnitude, possibly larger than the physical forcing terms, thereby violating the assumption that the artificial nudging terms should not be a dominant forcing in the model equations.

Table 2 shows the results of using these average (frozen) hybrid nudging-EnKF coefficients in the second 3000-step period. The average RMS analysis errors of FHNKFx and FHNKDx are smaller than those of TNGAx (except for FHNKD8 and FHNKD4). So the off-diagonal terms helped to produce RMS errors that were still smaller than those using traditional nudging, but these errors were still larger than those using the EnKF through this period, as expected. Thus the historical hybrid nudging-EnKF coefficients in the previous 3000 time steps may have some value in the next 3000 time steps. This suggests that after integrating the ensemble forecast and calculating the EnKF gain matrix once, the average hybrid nudging-EnKF coefficients, especially the full matrix, can be determined and applied in the future. This is the same general idea used in some calibrations of ensemble forecasts that apply corrections from the recent past to future forecasts (Raftery et al. 2005).

RMS analysis error in the traditional nudging scheme increases with decreasing the half-period of the nudging time window (from x = 8 to x = 1). Results of TNGA1 with the same nudging coefficients as TNGA2, TNGA4, and TNGA8 had

minimal impact as expected because decreasing the nudging time window reduces the time that the system is gradually forced by the observations, which in turn reduces the impact of the observations. However, there is not a simple linear relationship for the average RMS analysis error with the half-period of nudging time window in the two hybrid nudging-EnKF schemes. As shown in Table 1, the RMS error first decreases with decreasing nudging time window and then increases in HNKFx experiments, and the error in HNKDx experiments decreases first then increases, and decreases again. Thus, the nudging coefficient provided by the EnKF gain matrix results in a nonlinear response of the average RMS error to the nudging time window. This may be due to the highly nonlinear Lorenz system and the calculation of EnKF gain matrix, and the possibility that large nudging coefficients decouple the model equations.

All of the previous experiments used an observation density of one per 25 time steps, and we computed the RMS errors against the truth state every time step. Now we investigate the effects of different observation densities (one per 10 time steps and one per 50 time steps) for traditional nudging and both hybrid methods. Similarly the average RMS analysis error in the traditional nudging scheme (TNGA4) increases while the observation density in time is reduced, as shown in Fig. 2a. Figures 2b and 2c show that the two hybrid nudging-EnKF schemes (HNKF4 and HNKD4) have similar relationships to the observation density with the traditional nudging scheme, but the difference between the results using an observation density of one per 25 time steps and one per 10 time steps in the two hybrid nudging-EnKF schemes is much smaller than that in the traditional nudging scheme. It appears that the

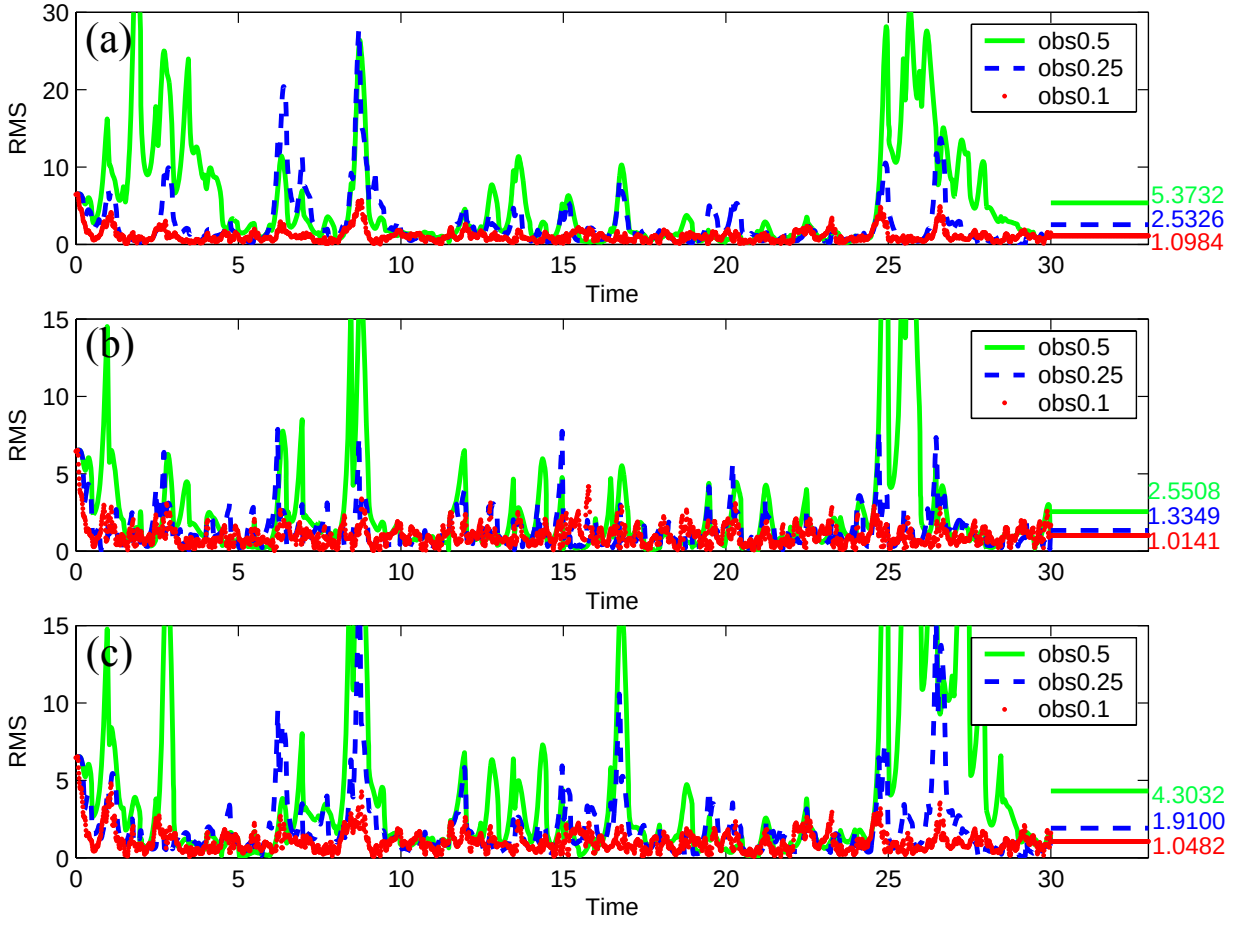

Figure 2. The RMS error during the first 3000-step period of (a) TNGA4, (b) HNKF4 and (c) HNKD4 with different observation densities. The solid green line denotes an observation density of one per 50 time steps (obs0.5), the dashed blue line indicates an observation density of one per 25 time steps (obs0.25), and the dotted red line represents an observation density of one per 10 time steps (obs0.1). The horizontal lines and values on the right side of the figure denote the average RMS error during the first 3000-step period.

accuracy of the simulated hybrid nudging state using the full matrix is less sensitive to the observation density than the other two nudging experiments. Figure 2 also shows that the RMS error in the two hybrid nudging-EnKF approaches are smaller than that in the traditional nudging approach given the same observation density, and the RMS error in the hybrid nudging-EnKF with the full nudging magnitude matrix is the smallest of all three experiments.

Since the hybrid nudging-EnKF approaches use the EnKF gain matrix to provide nudging coefficients that produce smaller RMS errors in the model, the underlying assumption for nudging stated by Stauffer and Seaman (1990; 1994) that the nudging terms should be constrained to be smaller than the model's physical terms in order to retain the physical properties and dynamic balance / intervariable consistency of the system may be violated. Figure 3 shows the average ratios of the nudging terms over the sum of the physical terms in each equation in the first 3000-step period of experiment HNKF4. The ratios of the y nudging term in the x-equation and the x and y nudging terms in the y-equation are less than 0.5 but larger than 0.1 (an order of magnitude difference in the magnitudes of the nudging and physical terms). The other nudging terms have ratios smaller than 0.1. In other words, the time scale of the nudging term (1/G) should be larger than that of the smallest physical terms in the model, on average. Otherwise, the artificial nudging forcing will disrupt the natural balance of forces within the model, which diminishes the role of the model equations in the data assimilation.

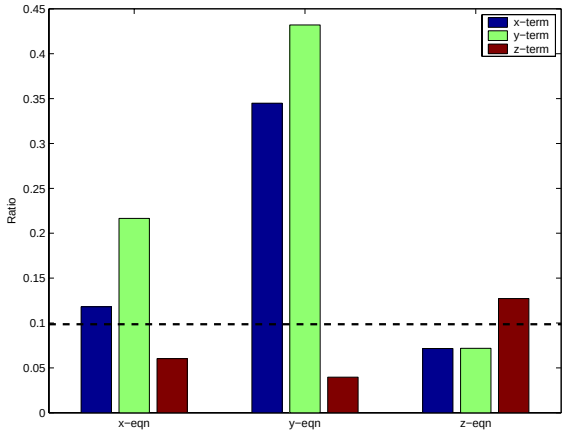

Figure 3. The ratios of the nudging terms compared to the physical terms averaged over the first 3000-step period in each equation in HNKF4. The dashed line denotes a ratio of 0.1, where the nudging term is an order of magnitude smaller than the sum of the physical forcing terms.

In contrast to the synchronization of the master (truth run) with the slave (model with coupling/nudging terms) in Yang et al. (2006) and the use of some intermittent assimilation strategies, atmospheric data assimilation schemes that make small corrections to the model background to correct the model trajectory minimize the insertion noise and maximize the natural dynamic balance within the nudged model state. Thus complete success with any nudging approach in the atmospheric sciences should require that the magnitude of the nudging terms be constrained relative to the physical forcing terms, so that dynamic balance and consistency are retained in addition to reducing the RMS errors compared to the truth state. A nudging period which is too short may cause the nudging coefficients / nudging strength to become too large relative to the other forcing terms, and create numerical noise and data rejection.

Another measure of success for a data assimilation scheme in NWP is to improve the forecast. For example, it is important to know if the hybrid nudging-EnKF approach with the full nudging magnitude matrix is also effective in providing a better forecast. From above, the hybrid nudging-EnKF approach with only the diagonal elements of the nudging magnitude matrix has similar or smaller RMS errors than traditional nudging but larger RMS errors than the hybrid nudging-EnKF approach with the full nudging magnitude matrix. So here we discuss the hybrid nudging-EnKF approach with the full nudging magnitude matrix applied to the dynamic initialization problem.

Figure 4 shows the results of dynamic initialization on EKFA, TNGA4 and HNKF4, respectively. The scale of the nudging coefficients is 10 as shown in Fig. 1, so the e-folding time is 0.1. Since the minimum time needed for effective nudging is generally 2 or 3 e-folding times, assuming that this period is less than the error correlation time scale, the pre-forecast dynamic-initialization period is chosen here as 5, 10 and 20 e-folding times. This is the same as assimilating 3, 5 and 9 observations with the observation density of one per 25 time steps. The results of the hybrid nudging-EnKF (Fig. 3g-3i) are similar with those of EnKF (Fig. 3a-3c) owing to the use of EnKF gain matrix. Comparing Fig. 3a, 3d, 3g using 20 e-folding times to the others, assimilating more observations during a longer pre-forecast period does not lead to better forecasts necessarily. Assimilating 5 observations (10 e-folding times) in each data assimilation scheme obtains the best forecast (Fig. 3b, 3e and 3h). The dynamic initialization experiments appear to be most effective at producing a better forecast than the FCST for a time period of 2 to 3 at best. In this time period, HNKF4 and EKFA produce a better forecast than

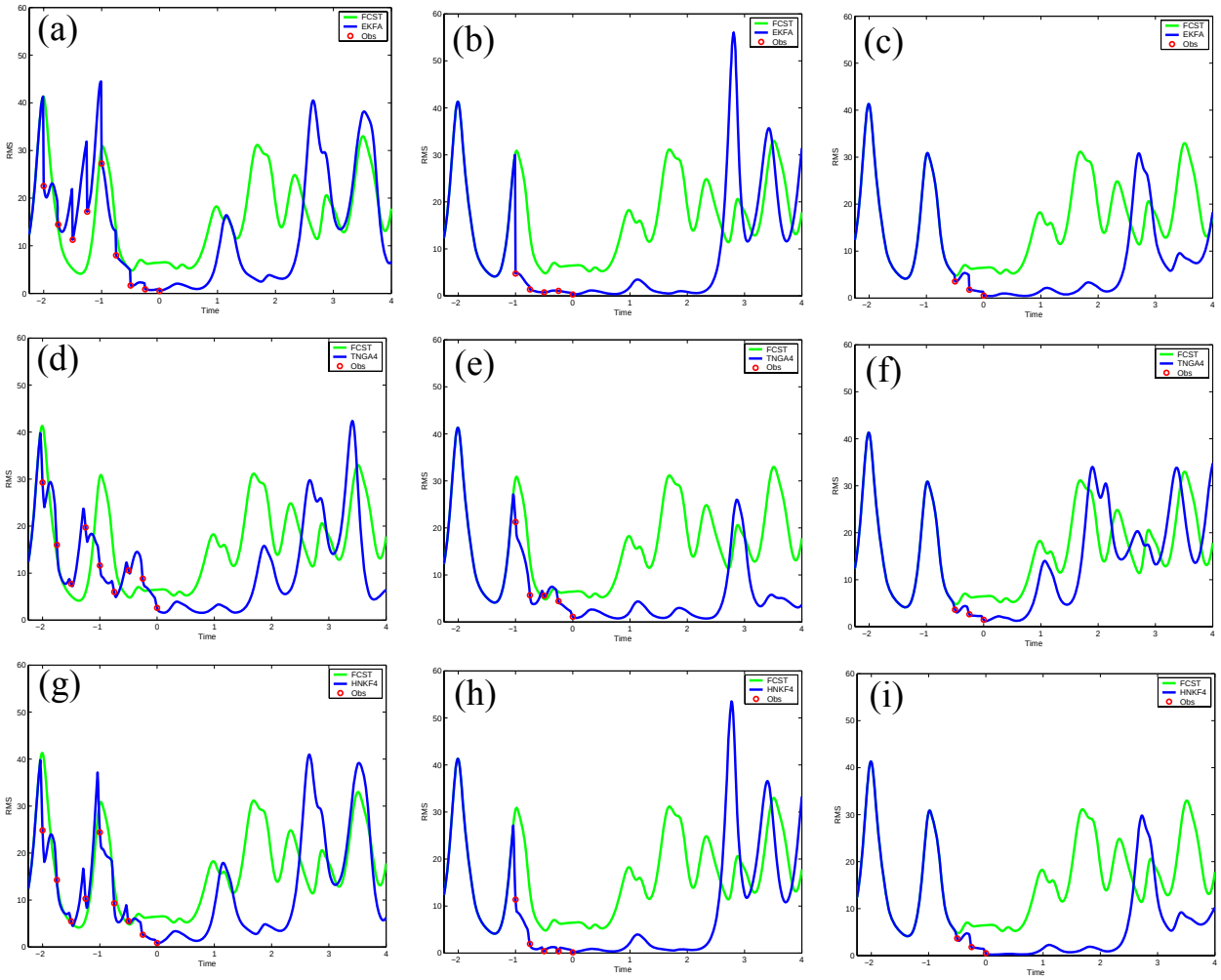

Figure 4. The RMS error as a function of time during the dynamic-initialization period and subsequent forecast with different data assimilation schemes and various lengths for the dynamic-initialization period in terms of e-folding times (1/G). EKFA: (a) 20 e-folding times, (b) 10 e-folding times, (c) 5 e-folding times; TNGA4: (d) 20 e-folding times, (e) 10 e-folding times, (f) 5 e-folding times; HNKF4: (g) 20 e-folding times, (h) 10 e-folding times, (i) 5 e-folding times. The green line is the RMS error of FCST (no assimilation of observations), which is the same in every figure, the blue line is the RMS error of each experiment using data assimilation during a pre-forecast dynamic-initialization period followed by a free forecast, and the circles denote the times of observations used in the pre-forecast assimilation.

TNGA4 except for the longest pre-forecast period assimilating 9 observations. Thus the hybrid nudging-EnKF is also more effective at improving the forecast accuracy in this case using dynamic initialization than the traditional nudging method over the shorter pre-forecast periods. Traditional nudging outperformed the hybrid method for the longest pre-forecast period. Although these results may change with different time windows, initial conditions, and observation densities, the hybrid nudging-EnKF approach also appears to be effective for model initialization and improved short-term forecasting. These results suggest that the length of the pre-forecast period must be chosen very carefully in highly nonlinear cases.

5. SUMMARY

A hybrid nudging-EnKF approach with potential use for NWP was explored here, which allows the EnKF to provide flow-dependent / time-varying error covariance to compute the nudging coefficients rather than using ad-hoc nudging coefficients derived from theory and experience. Traditional multiscale nudging methods (Stauffer and Seaman 1994) have been proven to be very effective and efficient for mesoscale NWP nowcasting (Stauffer et al. 2007a) and forecasting (Stauffer et al. 2007b) applications. In the former, multiscale nudging is used in a model forecast for current

conditions (called a "nowcast"), available just ahead of the clock and continuously assimilating standard and special observations as the model integrates forward in time to provide high quality meteorological information for Army and Marines Corps use. In the latter, a "running start" dynamic initialization using multiscale nudging of standard and special observations at 36-km, 12-km, 4-km and 1.3-km horizontal model resolutions over the complex terrain of the Italian Alps and Torino plains for the 2006 Winter Olympics, produced improved initial conditions and subsequent 24-h forecasts for the Department of Defense for hazard prediction and consequence assessment. The model cloud, precipitation and local circulations were spunup at the initial time, which improved the short-term forecasts. The nudging magnitude and weighting functions were based on theory and past experience including terrain considerations.

This hybrid nudging-EnKF approach explored here contributed to a more rapid assimilation of the data and a better fit of an analysis to the data (decreased RMS errors compared to the truth), and improved forecasts, than the traditional nudging data assimilation scheme. This is promising because the hybrid method also accounts for model background error based on ensemble spread, and observation errors. However, the magnitude of the hybrid nudging coefficients should be constrained so that the nudging terms are smaller than the physical terms in the model equations on average, so that the time scale for the nudging term is longer than that of the smallest physical terms in the model (e.g., Stauffer and Seaman 1990).

A set of temporally averaged hybrid nudging-EnKF coefficients was obtained during a historical period using the hybrid nudging-EnKF approach. These temporally averaged hybrid nudging-EnKF coefficients were found to have added value in a future period for analysis. Therefore, archived hybrid nudging-EnKF coefficients may provide some useful statistical information for defining the nudging coefficients during the dynamic initialization period for future forecast applications since the EnKF can be quite expensive in real-time NWP applications. This work with a "toy" model representing a highly nonlinear system such as the atmosphere serves as a test bed for further experimentation in more sophisticated models such as a shallow water model and three-dimensional mesoscale model. These results offer a proof of concept that will be further analyzed and used to begin development and testing of a hybrid nudging-EnKF in the Weather Research and Forecast (WRF) model.

6. ACKNOWLEDGMENTS

This research is supported by DTRA contract no. HDTRA1-07-C-0076. The authors would like to thank Sue Ellen Haupt and George S. Young for helpful discussions and comments.

7. REFERENCES

Evensen, G., 1994: Sequential data assimilation with a nonlinear quasi-geostrophic model using Monte Carlo methods to forecast error statistics. *J. Geophys. Res.*, **99(C5)**, 10143-10162.

Kalata, P. R., 1984: The tracking index: A generalized parameter for α-β and α-β-γ target trackers. *IEEE transactions on aerospace and electronic systems,* **AES-20**, 174-182.

Lorenz, E., 1963: Deterministic non-periodic flow. *J. Atmos. Sci.,* **20**, 130-141.

Painter, J. H., D. Kerstetter, S. Jowers, 1990: Reconciling steady-state Kalman and Alpha-Beta filter design. *IEEE transactions on aerospace and electronic systems,* **26**, 986-991.

Stauffer, D. R., and N. L. Seaman, 1990: Use of four-dimensional data assimilation in a limited-area mesoscale model. Part I: Experiments with synoptic data. *Mon. Wea. Rev.,* **118**, 1250-1277.

Stauffer, D. R., and J.-W. Bao, 1993: Optimal determination of nudging coefficients using the adjoint equations. *Tellus,* **45A**, 358-369.

Stauffer, D. R., and N. L. Seaman, 1994: Multiscale four-dimensional data assimilation. *J. Appl. Meteor.,* **33**, 416-434.

Stauffer, D.R., A. Deng, G.K. Hunter, A.M. Gibbs, J.R. Zielonka, K. Tinklepaugh, and J. Dobek, 2007a: NWP goes to war …, 22nd Conference on Weather Analysis and Forecasting/18th Conference on Numerical Weather Prediction, June 25-29, Park City, UT.

Stauffer, D.R., G.K. Hunter, A. Deng, J.R. Zielonka, K. Tinklepaugh, P. Hayes, and C. Kiley, 2007b: On the role of atmospheric data assimilation and model resolution on model forecast accuracy for the Torino Winter Olympics, 22nd Conference on Weather Analysis and Forecasting/18th Conference on Numerical Weather Prediction, June 25-29, Park City, UT.

Raftery, A. E., T. Gneiting, F. Balabdaoui, and M. Polakowski, 2005: Using Bayesian model averaging to calibrate forecast ensembles. *Mon. Wea. Rev.,* **133**, 1155-1174.

Yang, S., D. Baker, H. Li, K. Cordes, M. Huff, G. Nagpal, E. Okereke, J. Villafane, E. Kalnay, and G. Duane, 2006: Data Assimilation as synchronization of truth and model: experiments with the three variable Lorenz system. *J. Atmos. Sci.,* **63**, 2340-2354.